Article

Cell Reports

Structural and Functional Analysis of the Cdk13/Cyclin K Complex

Graphical Abstract

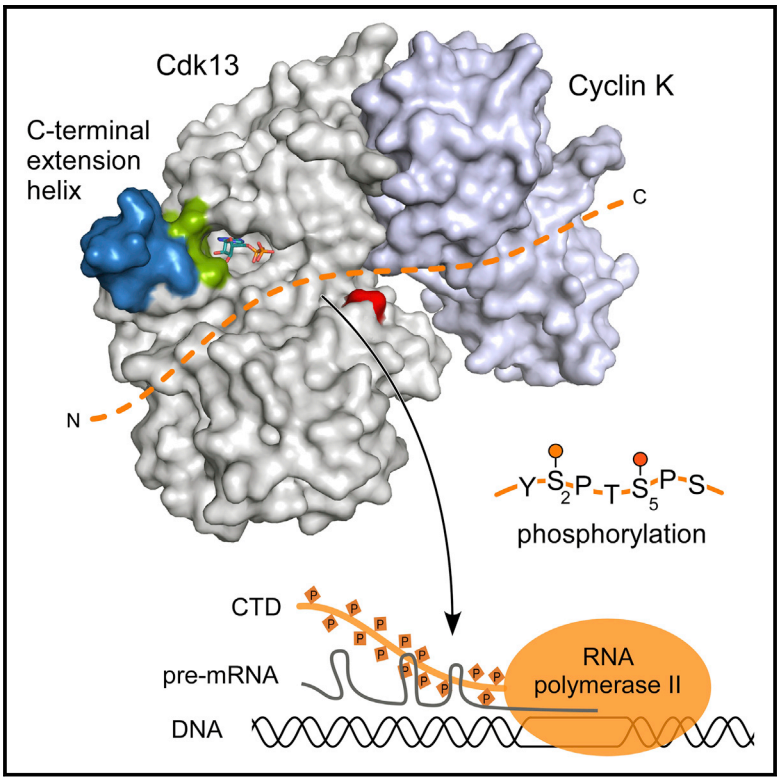

Authors

Ann Katrin Greifenberg, Dana Hönig, Kveta Pilarova, ..., Kanchan Anand, Dalibor Blazek, Matthias Geyer

Correspondence

geyer@uni-bonn.de

In Brief

Cyclin-dependent kinases regulate transcription through phosphorylation of RNA polymerase II. Greifenberg et al. report the structure of the human Cdk13/Cyclin K complex. Cdk13 contains a C-terminal extension helix that is a specific feature of transcription elongation kinases.

Highlights

- The crystal structure of the human Cdk13/Cyclin K complex
- Cdk13 phosphorylates Ser5 and Ser2 of the RNA polymerase II CTD
- The isomerase Pin1 does not change the phosphorylation specificity of Cdk13
- Cdk13 regulates genes involved in growth signaling pathways

Accession Numbers

5EFQ

Greifenberg et al., 2016, Cell Reports *14*, 320–331
January 12, 2016
http://dx.doi.org/10.1016/j.celrep.2015.12.025

OPEN ACCESS
CellPress

Cell Reports
Article

Structural and Functional Analysis of the Cdk13/Cyclin K Complex

Ann Katrin Greifenberg,[1,2] Dana Hönig,[2,3] Kveta Pilarova,[4] Robert Düster,[1,2] Koen Bartholomeeusen,[4] Christian A. Bösken,[2,3] Kanchan Anand,[1,5] Dalibor Blazek,[4] and Matthias Geyer[1,2,3,*]

[1]Institute of Innate Immunity, Department of Structural Immunology, University of Bonn, Sigmund-Freud-Strasse 25, 53127 Bonn, Germany
[2]Center of Advanced European Studies and Research, Group Physical Biochemistry, Ludwig-Erhard-Allee 2, 53175 Bonn, Germany
[3]Max Planck Institute of Molecular Physiology, Department of Physical Biochemistry, Otto-Hahn-Strasse 11, 44227 Dortmund, Germany
[4]Central European Institute of Technology (CEITEC), Masaryk University, 62500 Brno, Czech Republic
[5]Present address: EMBL Heidelberg, Structural and Computational Biology Programme, Meyerhofstrasse 1, 69117 Heidelberg, Germany
*Correspondence: geyer@uni-bonn.de
http://dx.doi.org/10.1016/j.celrep.2015.12.025

SUMMARY

Cyclin-dependent kinases regulate the cell cycle and transcription in higher eukaryotes. We have determined the crystal structure of the transcription kinase Cdk13 and its Cyclin K subunit at 2.0 Å resolution. Cdk13 contains a C-terminal extension helix composed of a polybasic cluster and a DCHEL motif that interacts with the bound ATP. Cdk13/CycK phosphorylates both Ser5 and Ser2 of the RNA polymerase II C-terminal domain (CTD) with a preference for Ser7 pre-phosphorylations at a C-terminal position. The peptidyl-prolyl isomerase Pin1 does not change the phosphorylation specificities of Cdk9, Cdk12, and Cdk13 but interacts with the phosphorylated CTD through its WW domain. Using recombinant proteins, we find that flavopiridol inhibits Cdk7 more potently than it does Cdk13. Gene expression changes after knockdown of Cdk13 or Cdk12 are markedly different, with enrichment of growth signaling pathways for Cdk13-dependent genes. Together, our results provide insights into the structure, function, and activity of human Cdk13/CycK.

INTRODUCTION

Higher organisms have evolved a unique structure in the RNA polymerase II (RNAPII) to coordinate transcription and the attendant processing of pre-mRNA molecules. The largest subunit Rpb1 of RNAPII contains a C-terminal extension, termed the C-terminal domain, or CTD, which is composed of multiple repeats of the hepta-sequence $Y_1S_2P_3T_4S_5P_6S_7$. The number of repeats varies between 26 in yeast and 52 in humans and is thought to correlate with the genomic complexity of the organism (Buratowski 2009; Corden 2013; Eick and Geyer, 2013). In addition, alterations from the consensus sequence occur in higher eukaryotes with a change in position 7 from serine to lysine prevailing in the distal part of the human CTD. The repetitive structure of the CTD is thought to act as a binding scaffold for transcription associated factors. The five hydroxyl group containing residues Tyr1, Ser2, Thr4, Ser5, and Ser7 are all susceptible to post-translational modifications (PTMs) combined with a *cis/trans* isomerization of the two intermediate prolines, Pro3 and Pro6. The reversible modifications by phosphorylation or *O*-linked glycosylation as well as acetylation and methylation of basic residues open a plethora of possible combinations of PTMs, often described as RNAPII CTD code.

Phosphorylation of the three serine residues within the CTD is tightly linked to the phases of RNAPII-mediated transcription (Adelman and Lis, 2012). At first, the unphosphorylated polymerase is recruited into the pre-initiation complex at open chromatin structures. In a simplified model, phosphorylation of Ser7 (pSer7) starts the transcription cycle until an additional pause step stalls the polymerase about 50 nucleotides downstream of the transcription start site (TSS). To overcome this promoter proximal pausing, Ser5 is phosphorylated, potentially in conjunction with Ser7, leading to the robust elongation of transcripts. On a molecular level, Ser7 phosphorylation primes the CTD for further modifications (Czudnochowski et al., 2012; St Amour et al., 2012), but, whereas Ser7 phosphorylation levels stay high during the transcription process, the pSer5 signal decreases steadily toward the poly-adenylation site by the action of phosphatases. Ser2 phosphorylation instead increases toward the transcription termination site (TTS), consistent with the recruitment of 3′ RNA-processing factors by pSer2 marks (Davidson et al., 2014). The phosphorylation signals are removed by phosphatases during the termination process, giving way for a new transcription cycle of the polymerase.

Cyclin-dependent kinases (CDKs) play major roles in the regulation of the cell cycle and transcription. Five mammalian CDKs have been described to date as transcription regulating kinases together with their corresponding cyclin subunits: Cdk7/Cyclin H as components of the general transcription factor TFIIH (Grünberg and Hahn, 2013), Cdk8/Cyclin C as components of the Mediator kinase module (Allen and Taatjes, 2015), Cdk9/Cyclin T1 or T2 that constitute the active form of the positive transcription elongation factor (P-TEFb) (Peterlin and Price, 2006), and Cdk12/Cyclin K and Cdk13/Cyclin K as the latest members of RNAPII CTD kinases (Bartkowiak et al., 2010; Blazek et al., 2011). A precise assignment of the various CDKs to the different

serine phosphorylations within the transcription cycle is not yet clear, as some promiscuity in the specificity of the kinases persists. However, Cdk9 is commonly described as a transcription elongation kinase that is located at the TSS in line with its function to overcome the promoter proximal arrest (Ghamari et al., 2013). Cdk7 in contrast initiates transcription, both by phosphorylating Ser7 of the CTD and by its ability to phosphorylate the activating threonine in the T-loop of CDKs (Larochelle et al., 2012).

Human Cdk12 and Cdk13 are large proteins with molecular weights of 164 and 165 kDa, respectively. The proteins share 43% sequence identity and harbor a central kinase domain. In contrast to CDKs 7, 8, and 9, human kinases Cdk12 and Cdk13 contain expanded regions of serine-arginine (SR) motifs in their N-terminal regions. These regions span residues 130–380 in Cdk12 and 200–435 in Cdk13, respectively, linking the kinases to the SR protein family involved in RNA processing and pre-mRNA splicing (Zhou and Fu, 2013; Ghosh and Adams, 2011). Accordingly, Cdk13 was demonstrated to interact with the splicing factor SRSF1 and to regulate alternative splicing of HIV (Berro et al., 2008). Cdk12 in turn was shown to regulate DNA-damage response genes and somatic gene mutations of the kinase were found in multiple cancers as high-grade serous ovarian carcinoma (The Cancer Genome Atlas Research Network, 2011; Ekumi et al., 2015; Joshi et al., 2014). However, the exact roles of Cdk13 and Cdk12 in these processes are yet to be explored.

In an effort to understand the molecular basis of Cdk13 function, we determined the crystal structure of the kinase/cyclin domains of human Cdk13/CycK at 2.0 Å resolution. Cdk13 contains a C-terminal extension helix following the canonical kinase domain that interacts with the bound ATP substrate. Flavopiridol is a poor inhibitor of Cdk13 activity but inhibits Cdk7 more potently, explaining its potency in downregulating transcription associated processes. The *cis/trans* peptidyl-prolyl isomerase Pin1 does not change the phosphorylation specificity of Cdk13/CycK for Ser5 and Ser2 sites, while pre-incubation of a CTD substrate with Cdk9 showed a small increase in Cdk13 activity. Finally, we find that Cdk13 and Cdk12 regulate different sets of genes, with Cdk13 activity mostly involved in growth signaling pathways.

RESULTS

Structure of the Cdk13/Cyclin K Complex

Human Cdk13 is an unusually large kinase that harbors a central kinase domain flanked by an N-terminal SR region and a C-terminal region of low complexity (Figure 1A). Its corresponding cyclin partner CycK contains a cyclin-box domain followed by a wide-stretched proline-rich region with 42% proline content over 220 amino acids. For structure determination, the kinase and cyclin box domains of human Cdk13/CycK were expressed in baculovirus infected insect cells co-transfected with the CDK activating kinase CAK1 from *S. cerevisiae*. The complex was purified to homogeneity by affinity chromatography and gel filtration analysis (Figure S1). Crystals were grown in the presence of ADP, aluminum fluoride, and the substrate peptide P-pS-YSPTSP-pS-YSPT by the hanging drop diffusion technique (see Experimental Procedures). The crystallographic phases were solved by molecular replacement with the coordinates of Cdk12/CycK as a search model and the structure was determined to a resolution of 2.0 Å. The protein complex was refined to an R_{work} of 19.5% and R_{free} of 24.7% with excellent stereochemistry (Table S1). Two Cdk13/CycK heterodimers form the asymmetrical unit cell of the protein crystal. No crystallographic density was observed for the substrate peptide but only for the AlF_3 transition state mimic and two magnesium ions (Figure 1B).

Cdk13 exhibits the typical kinase fold consisting of an N-terminal lobe (aa 695–794) and a C-terminal lobe (aa 795–998) that share 46.9% sequence identity to Cdk9 and 41.4% sequence identity to Cdk2, respectively. The orientation of the αC helix, also known as the ^{746}PITAIRE helix (Figures 1B and 2), is in the kinase active conformation, mediating contacts to the cyclin subunit. The ^{855}DFG motif at the start of the activation segment and the activation segment itself adopt conformations that allow access of the substrate to the catalytic site. Following the DFG motif is a leucine, L858, indicative for the preference of a SP motif rather than a TP motif for phosphorylation (Chen et al., 2014a). Similar to Cdk12, Cdk13 contains a C-terminal extension segment (aa 999–1032) following the canonical cyclin box domain that associates to the kinase domain (Figure 1C). A histidine and a glutamate residue within this stretch, H1018 and E1019, form water-mediated interactions to the ribose of the bound nucleotide (Figure 1D). The interactions of this central HE motif to the kinase domain are complemented by flanking residues D1016 and L1020 that weakly interact with the N- and C-terminal lobes of the kinase domain. The ^{1016}DCHEL sequence is succeeded by the polybasic region ^{1023}KKRRRQK, which is resolved in the second chain of Cdk13 up to M1031, thought without displaying electron density for the side chains of the positively charged amino acids (Figure S2). Its conformation reveals that the HE motif and the polybasic cluster form a continuous helix adjacent to the kinase active center.

Cdk/Cyclin Complexes of Transcription Elongation Kinases Adopt an Open Conformation

The orientation of the cyclin subunit with respect to the kinase domain is rotated in Cdk13/CycK by 21° toward an open conformation compared to the structure of Cdk2/CycA (Figure 3A). This leads to exposure of the kinase active center as the first cyclin-box domain of CycK is bent apart from the kinase T-loop element. A similar arrangement has been observed for the Cdk9/CycT1 complex and the Cdk12/CycK complex with rotations of 26° and 24°, respectively, compared to Cdk2/CycA (Figure 3B). One explanation for the twist of the two subunits with respect to each other is that the phospho-threonine in the T-loop segment of the kinase is coordinated only by two of the three canonical arginine residues (Figure 2). Phospho-T871 within the activation segment is clearly visible in the electron density map and forms salt bridges with R836 and R860 (Figure 3C). The third canonical arginine residue instead, R751 of the PITAIRE motif, is about 8.1 Å apart from the phosphate group. It forms an intermolecular salt bridge with the second glutamate of the ^{105}KVEE motif in CycK, which is conserved in cyclins C, H, K, and T (Figure S3). These four cyclins are the corresponding subunits to transcription regulating kinases

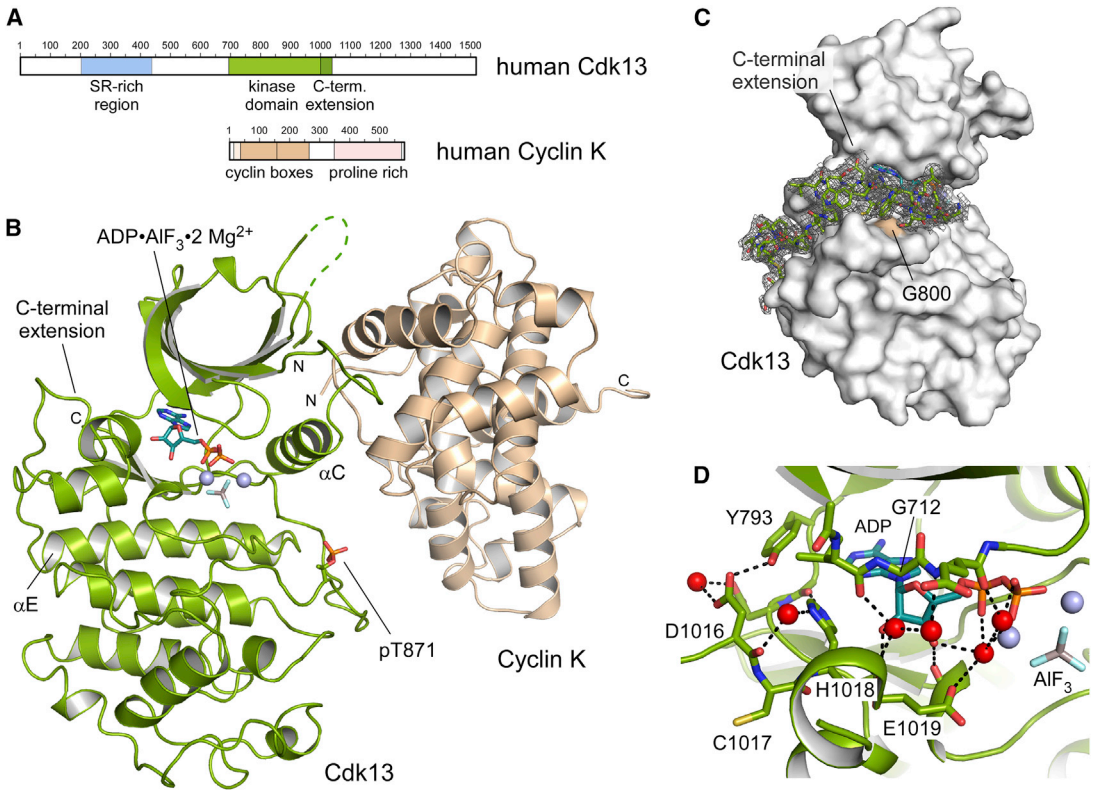

Figure 1. Structure of the Human Cdk13/CycK Complex

(A) Domain architectures of human Cdk13 (UniProt: Q14004) and human Cyclin K (O75909). Cdk13 contains an extended N-terminal serine-arginine (SR)-rich region that spans 250 amino acids, followed by the central kinase domain. Human CycK consists of an N-terminal cyclin box domain followed by a region of low complexity of more than 300 amino acids, containing more than 35% prolines.

(B) Overall structure assembly of Cdk13 (green) and CycK (beige). The ADP•AlF_3 nucleotide and the phospho-threonine residue in the T loop segment of the kinase are highlighted.

(C) Coordination of the C-terminal extension in Cdk13 following the canonical kinase domain. Residues 1001–1024 are shown as cartoon with the final $2F_o$–F_c electron density displayed at 1σ. The structure of the Cdk13 kinase domain is shown as surface representation.

(D) Close up of the interactions of the C-terminal extension helix with the kinase domain and the bound nucleotide. H1018 and E1019 of the DCHEL motif in Cdk13 form water-mediated contacts to ADP complemented by interactions of D1016 with residues of the N- and C-terminal kinase lobes.

Cdk8, 7, 12 and 13, and 9. A similar arrangement to Cdk13/CycK is found in Cdk12/CycK, where the arginine residue of the PITAIRE motif solely forms intermolecular interactions with the cyclin subunit (Bösken et al., 2014). The arginine of the PITALRE sequence in Cdk9/CycT1 instead contacts both the phospho-threonine of the T-loop and the second glutamate of the KVEE motif (Schulze-Gahmen et al., 2013). For comparison, the three canonical arginines R50, R126, and R150 of Cdk2 all form tight salt bridges with the phospho-threonine pT160 (Russo et al., 1996), with R50 of the PSTAIRE helix interacting additionally with the first glutamate of the KFEE motif in Cyclin A (Figure 3D).

The orientation of the two subunits relative to each other is reflected by the size of the buried surface area of the Cdk/cyclin complexes. Whereas the buried surface area of Cdk2/CycA involves both kinase lobes and cyclin boxes and encompasses 3,286 $Å^2$ (PDB:1JST) when counting both subunits, the Cdk13/CycK interface of 2,002 $Å^2$ involves only the N-terminal lobe of the kinase and the first cyclin box repeat. Likewise, Cdk12/CycK covers a buried surface area of 2,161 $Å^2$ (PDB: 4NST) and those of Cdk9/CycT1 1,819 $Å^2$ only (PDB: 3BLQ). The smaller interfaces thus correlate with the open conformation of the Cdk/cyclin subunits, which appears as a common feature of transcription elongation kinases. A detailed view on the molecular interface between Cdk13 and CycK is shown in Figure S4.

Cdk13 Is a Promiscuous Kinase for RNAPII CTD Phosphorylations

We tested the activity of the Cdk13/CycK complex both for its substrate recognition preference as well as for the phosphorylation specificity of the substrate. A series of synthetic CTD peptides was analyzed, each containing three hepta repeats followed by a polyethylene linker and two arginines. Besides the consensus sequence, peptides uniformly phosphorylated at positions Tyr1, Ser2, Thr4, Ser5, and Ser7 were used as well as a Lys7 variant (Itzen et al., 2014). Cdk13/CycK showed the highest activity on the pre-phosphorylated pSer7-CTD substrate, whereas the non-phosphorylated consensus CTD peptide was poorly recognized (Figure 4A). pThr4-, pSer2-, and pTyr1-CTD peptides were all phosphorylated to a rather low

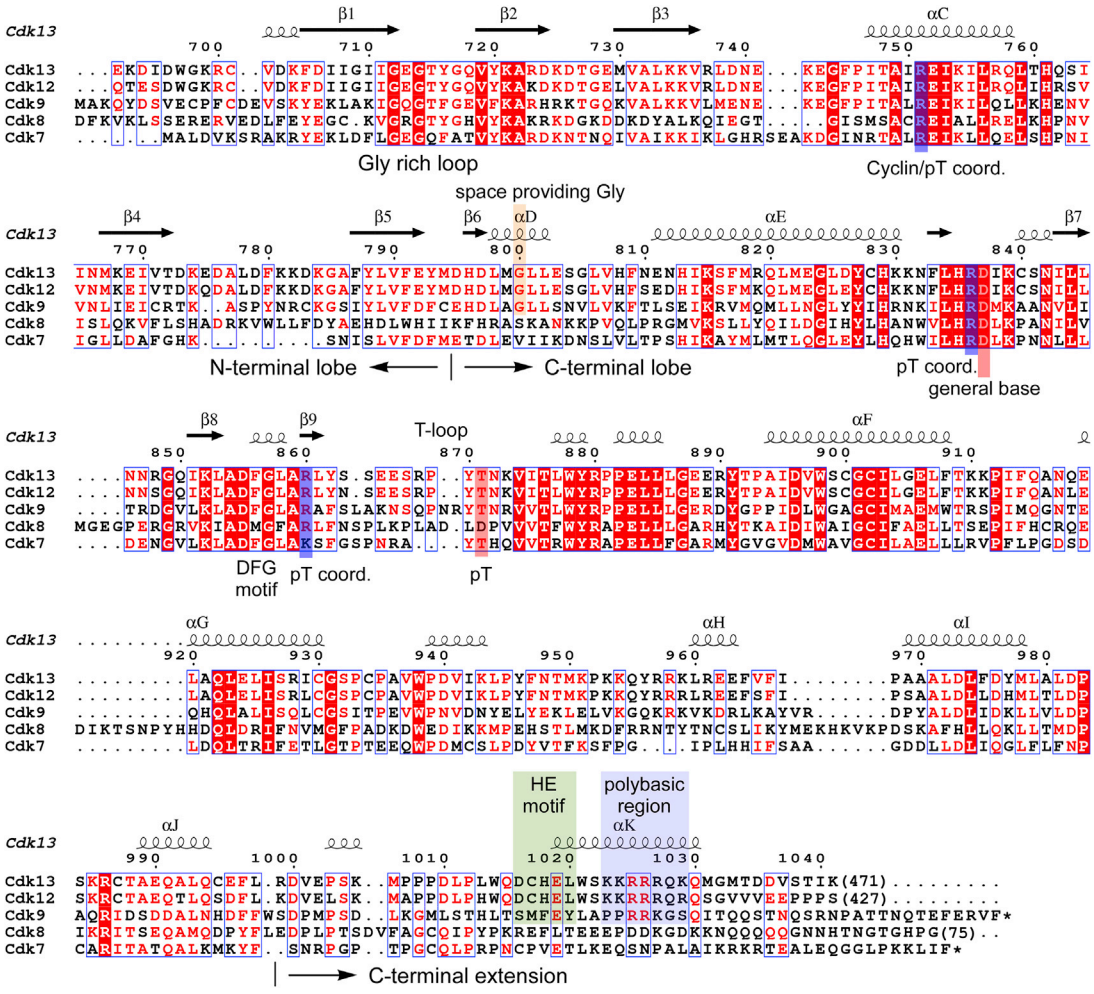

Figure 2. Sequence Alignment of Transcriptional CDKs

Sequence alignment of the kinase domains of human Cdk proteins involved in the regulation of transcription by RNA polymerase II. Secondary structure elements are indicated for Cdk13 as determined here. The HE motif and the polybasic cluster in the C-terminal extension helix αK present in the transcription elongation regulating kinases Cdk9 (UniProt: P50750), Cdk12 (UniProt: Q9NYV4), and Cdk13 are highlighted. The presence of these motifs correlates with a glycine residue in helix αD (G800) that provides space of the assembly of the extension helix with the bound nucleotide. Accession numbers for Cdk8 and Cdk7 are as follows: (UniProt: P49336 and P50613). Residues conserved in all CDKs are boxed red, and those that are similar are colored red. The sequence alignment was prepared with MultAlin; the secondary structure alignment was prepared with ESPript.

extent. The pSer5-CTD template and the K7-CTD peptide instead were not recognized for phosphorylations.

In a following experiment, single Ser2, Ser5, or Ser7 phosphorylation marks were placed in the N- or C-terminal repeat of the CTD peptide, giving insights into the direction and recognition specificity of the kinase. Only the peptide pre-phosphorylated at the C-terminal Ser7 position (pS7-C) was decently phosphorylated by Cdk13/CycK, albeit to less than 50% of the uniformly pSer7-CTD substrate control (Figure 4B). The five other single pre-phosphorylated peptides were phosphorylated to the same extent as the consensus CTD. These data suggest that the phosphorylation mark set by Cdk13/CycK is preferentially attached N-terminal to an existing pSer7 site.

To determine the site of phosphorylation set by Cdk13/CycK, we performed western blot analysis using monoclonal antibodies generated against pSer2, pSer5, and pSer7 marks. In addition, the activity of native full-length proteins was compared with recombinant CDK proteins as domains outside the canonical kinase fold could contribute to the phosphorylation specificity. Flag-tagged full-length Cdk13 and Cdk12 with their corresponding CycK subunit and Cdk9 proteins were expressed in HCT116 cells as well as the kinase dead (KD) variants Cdk13 (D855N), Cdk12 (D877N), and Cdk9 (D167N), respectively. Incubation of GST-CTD with anti-flag immuno-precipitated Cdk13 revealed equally strong signals for Ser2 and Ser5 phosphorylation, whereas no Ser7 phosphorylation was detected (Figure 4C). A similar result was obtained for recombinant Cdk13/CycK showing the same phosphorylation specificity as the native proteins. Likewise, native and recombinant Cdk12/CycK complexes exhibited a similar specificity for Ser2 and Ser5 phosphorylations, but again no Ser7 marks were set. In contrast, flag-tagged immuno-precipitated full-length Cdk9 strongly phosphorylated

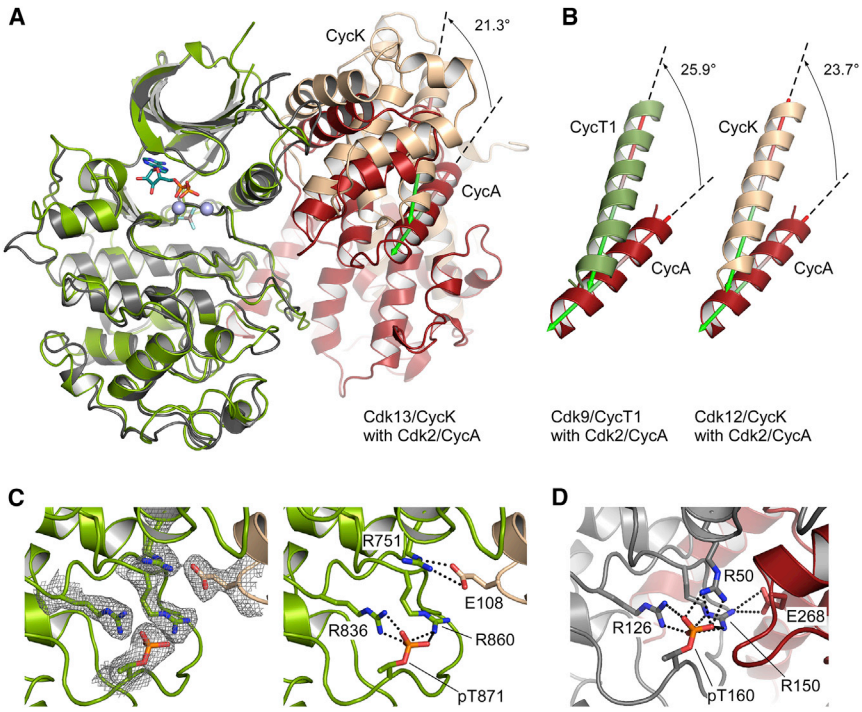

Figure 3. Transcription-Regulating Cdk/Cyclin Complexes Adopt an Open Conformation

(A) Superimposition of the two kinase subunits of the Cdk13/CycK complex (colored green/wheat, 5EFQ) and the Cdk2/CycA complex (gray/red, 1JST) reveals that the cyclin subunit of the Cdk13/CycK complex is twisted out toward an open conformation of the kinase active site. The orientation of helix H1 of the two cyclins is displayed by an arrow and the angle between the two helices given.

(B) Detailed view on the orientation of the first canonical helix H1 in CycT1 (left) and CycK (right) based on a superimposition of the kinase subunits in the Cdk/cyclin complexes Cdk9/CycT1 with Cdk2/CycA (3BLQ, 1JST) and Cdk12/CycK with Cdk2/CycA (4NST, 1JST). The cyclin subunits are twisted out by 26° and 24° relative to the kinase domains, suggesting that this assembly is a common feature of transcription elongation kinases.

(C) Close up of the phospho-threonine pT871 coordination in the Cdk13 T-loop segment. The final $2F_o–F_c$ electron density is displayed at 1σ (left). Ionic interactions are formed between the two canonical CDK arginines R836 and R860 and the phosphate group, whereas R751 of the PITAIRE sequence in helix C mediates electrostatic contacts with E108 of the ^{105}KVEE motif in CycK but is not directly contacting pT871.

(D) Salt bridge formation between the canonical arginines R50, R126, and R150, and the phosphate group of pT160 is a hallmark of CDK activation. This conformation arranges the cyclin subunit in a tight domain assembly.

Ser5 of the CTD and a little Ser7, but no Ser2 sites, similarly as observed before (Czudnochowski et al., 2012). The empty vector control and the kinase dead variants instead showed no phosphorylations of the CTD on Ser2 and Ser7 and severely reduced Ser5 phosphorylation intensity. Input controls by western blot analyses using anti-flag and anti-CycK antibodies confirm the integrity of the Cdk/cyclin complexes and display the amounts of kinases used in the in vitro kinase assays (Figure 4D). The contribution of the C-terminal extension helix to the kinase activity and specificity was probed by mutagenesis of the HE motif and the polybasic cluster (Figure S5). Both motifs were mutated to alanines, yet while the stability of the kinase was impaired for the HE mutant, the preferences for Ser5 phosphorylations of the full-length CTD remained unchanged.

Flavopiridol Inhibits Cdk7 More Potently Than It Does Cdk13

The small molecular compound flavopiridol is a widely used ATP competitive inhibitor of transcription elongation kinases (Baumli et al., 2008; Wang and Fischer, 2008). We tested its ability to inhibit Cdk13/CycK using recombinant proteins and the substrate pS7-CTD. To a concentration of 0.2 μM Cdk13/CycK and 1 mM ATP, flavopiridol was added in a concentration range from 3.1 nM to 310 μM. From a plot of the kinase activity versus the concentration of flavopiridol an in vitro IC_{50} value of 16.1 μM was determined, rendering flavopiridol a rather poor inhibitor of Cdk13 (Figure 5A). Intriguingly, structural analysis using the crystal structure of Cdk9 bound to flavopiridol (Baumli et al., 2008) superimposed with the structure of Cdk13 revealed a steric hindrance of flavopiridol with H1018 of the Cdk13 C-terminal extension helix (Figure 5B). The simultaneous occupancy of this site by flavopiridol and the HE motif of the extension helix is therefore precluded.

To further analyze the effect of flavopiridol in the inhibition of transcription processes, we tested its efficacy in the inhibition of Cdk7 kinase activity using recombinant protein. To a concentration of 0.2 μM Cdk7/CycH/MAT1, flavopiridol was added in increasing amounts from 1 nM to 100 μM concentration, using 1 mM ATP and 100 μM GST-$CTD_{[9]KKK}$ substrates. From a sigmoidal fit, an IC_{50} value of 2.3 μM was determined for the inhibition of Cdk7 by flavopiridol (Figure 5C). Flavopiridol thus inhibits Cdk7 more potently than it does Cdk13. This effect is remarkable given that Cdk7 is supposed to be the CDK activating kinase in mammals by its ability to phosphorylate the kinases T-loops (Larochelle et al., 2012).

The high efficacy of flavopiridol as transcription elongation inhibiting compound was further analyzed in cells. Using targeted small interfering RNAs (siRNAs), the expression levels of endogenous Cdk12 and Cdk13, respectively, were markedly reduced in HCT116 cells (Figure 5D). Yet, compared to the use of a randomized control siRNA, the changes in serine phosphorylation are very small. The use of flavopiridol, however, strongly diminished the phosphorylation levels of all three serines, indicating its broad inhibition of transcription processes.

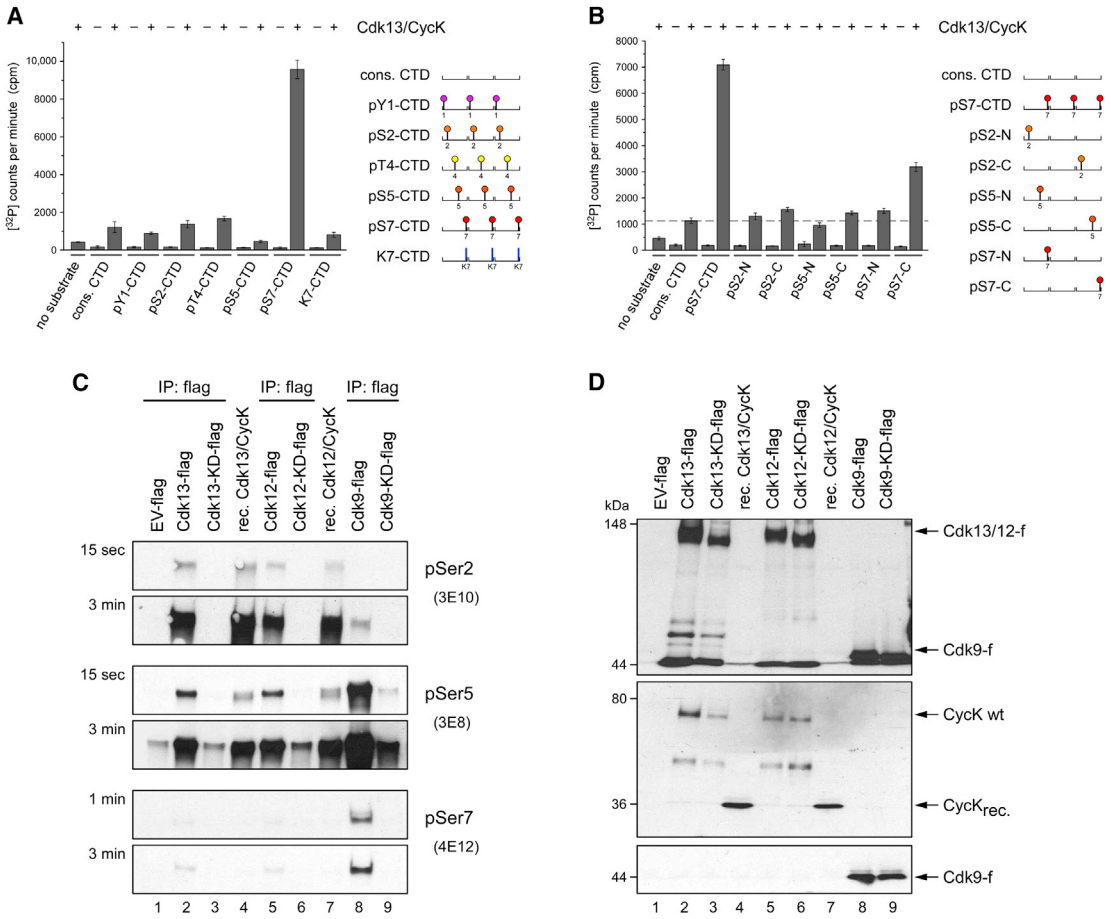

Figure 4. Substrate Preferences of Cdk13/CycK Phosphorylation

(A) Activity of Cdk13/CycK for a panel of CTD substrate peptides. Three hepta repeats with either no or continuous phosphorylation marks were provided. Cdk13 showed the highest activity for a peptide containing Ser7 pre-phosphorylations. Minor activities were detected for Thr4 and Ser2 pre-phosphorylated peptides and the consensus CTD, while no activity was seen on pSer5 and K7 peptides. A cartoon of the peptides used is shown on the right.

(B) Preferences of Cdk13 phosphorylations. Serine 2, 5, and 7 phosphorylations were set either in the N- or C-terminal repeat of a triple hepta-repeat substrate. Overall, the activity of Cdk13 toward these peptides is weak and only slightly above the consensus CTD. The substrate with the C-terminal pS7 mark gained the highest recognition preference. Data in (A) and (B) are reported as the mean ± SD of three independent experiments.

(C) In vitro kinase assays of Cdk13, Cdk12, and Cdk9 using GST-tagged full-length human CTD as substrate. Flag-tagged full-length kinases were immune-precipitated from HCT116 cells and compared to recombinant Cdk13 (673–1039)/CycK (1–267) or Cdk12 (696–1082)/CycK (1–267). After incubation, GST-CTD was subjected to western blot analysis using monoclonal antibodies (mAbs) specific for pSer2 (3E10), pSer5 (3E8), and pSer7 (4E12). EV, empty vector control; KD, kinase dead mutants. Exposure times are indicated on the left.

(D) Display of the protein input used in the in vitro kinase assays. Equal amounts of full-length proteins were used as shown by western blots with anti-flag (upper panel) and anti-CycK (middle panel) antibodies. Cdk13 purifications are free of Cdk9 contaminants as shown by western blot analysis with anti-Cdk9 antibody (lower panel).

Pin1 Does Not Change the Phosphorylation Preferences of Transcription Kinases

The CTD contains two serine-proline motifs within each consensus hepta repeat at positions 2/3 and 5/6, respectively. A characteristic feature of the prolyl-peptide bond is a slow rate of *cis/trans* isomerization (Schiene-Fischer et al., 2013). The 18-kDa Pin1 protein is a human peptidyl-prolyl *cis/trans* isomerase (PPIase) that binds to and isomerizes phosphorylated S/T-P (pSer/pThr-Pro) motifs (Hanes, 2014). It contains an N-terminal WW domain binding to pS and pT sites followed by the PPIase domain (Figure 6A). To analyze whether the presence of Pin1 affects the CTD phosphorylation mediated by transcription kinases Cdk13, Cdk12, or Cdk9, we performed in vitro kinase assays using 300 ng GST-CTD, 100 ng Pin1, and immuno-precipitated full-length kinases Cdk13-flag/CycK, Cdk12-flag/CycK, or Cdk9-flag/CycT1. For comparison, 100 ng of recombinant protein kinases Cdk13/CycK or Cdk12/CycK was used.

Using antibodies against either pSer2 or pSer5 marks, we find that the presence of Pin1 does not change the preferences of the full-length kinases for phosphorylating Ser5 (Figure 6B). The phosphorylation efficacy of the recombinant proteins Cdk13 and Cdk12, however, was markedly reduced upon addition of Pin1. This effect can be attributed to the presence of the WW

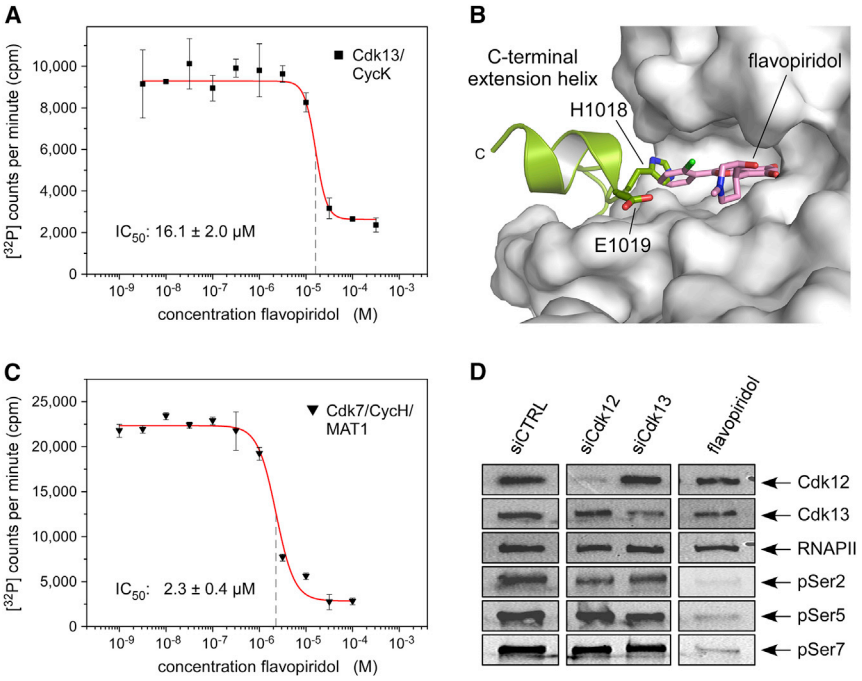

Figure 5. Flavopiridol Inhibits Cdk7 More Potently than Cdk13

(A) Concentration series of flavopiridol for the inhibition of Cdk13/CycK at 0.2 μM kinase concentration. The IC_{50} value was determined to 16.1 ± 2.0 μM against Cdk13 using pS7-CTD as a substrate.

(B) Model of the proposed position of flavopiridol in the ATP pocket of Cdk13. Flavopiridol clashes with the imidazole ring of H1018 in the C-terminal extension helix of Cdk13. The model is based on a superimposition of the Cdk9–flavopiridol structure (3BLR) with the structure of Cdk13 determined here.

(C) Concentration series of flavopiridol for the inhibition of Cdk7/CycH/MAT1 at 0.2 μM kinase concentration. The IC_{50} value was determined to 2.3 ± 0.4 μM against Cdk7, using a CTD template with nine hepta repeats. Data in (A) and (C) are reported as the mean ± SD from three independent experiments.

(D) Administration of flavopiridol leads to a decrease in RNA pol II serine phosphorylations. Flavopiridol was applied at 500 nM concentration to HCT116 cells. Depletion of Cdk12 and Cdk13 by siRNA, respectively, led to an approximate 2-fold decrease of Ser2 and Ser5 phosphorylations but did not affect Ser7 phosphorylation. Flavopiridol instead diminished all serine phosphorylations of the RNA pol II CTD, indicating its broad potency in the regulation of transcription kinases.

domain in Pin1 as deletion of the WW domain in the Pin1ΔWW protein variant restores the full kinase activity (Figure 6C). At the high molecular concentrations used in this experiment, the WW domain of Pin1 could mask the CTD for its recognition by the kinases. In a following experiment series, we tested whether pre-incubation of the CTD with Cdk9/CycT1 could change the ability of Cdk13 or Cdk12 to phosphorylate the CTD. Such effect could be a priming of the substrate for further modifications to determine, e.g., the succession of phosphorylation events in the transcription cycle. GST-CTD was pre-incubated for 20 min with immuno-precipitated Cdk9/CycT1 or a kinase dead variant of Cdk9. Pin1 was added optionally for 15 min before recombinant kinases Cdk13/CycK or Cdk12/CycK were subjected for another 40 min to the reaction. Again, a robust Ser5 phosphorylation was seen for Cdk9 in the pre-incubation time together with some Ser7 phosphorylation (Figure 6D, lanes 1 and 2). Addition of Cdk13/CycK or Cdk12/CycK led to additional Ser2 phosphorylation signals (lanes 3–6). Yet, compared to the Cdk9 kinase dead control assay (lanes 7–12), the intensity of the Ser2 phosphorylation bands were only 2- to 3-fold stronger. We therefore conclude that a small increase in Ser2 phosphorylation by transcription kinases Cdk12 and Cdk13 can be observed upon a priming step of the CTD with Cdk9. Addition of Pin1, however, not much influenced the kinase phosphorylation specificities observed in these experiments.

Gene Expression Changes after Knockdown of Cdk13 or Cdk12 Are Markedly Different

Given that the structures of the kinase domains of Cdk13 and Cdk12 are rather similar and that both kinases phosphorylate the CTD of RNAPII alike, we analyzed whether they also regulate the expression of a similar set of genes. To address this question, RNA expression profiling of HCT116 cells depleted of Cdk13 or Cdk12 was performed (Figure 7). Cells were transfected with control, Cdk13, or Cdk12 siRNAs in triplicate, and RNA was isolated after 72 hr for expression analyses. Knockdown efficacy was assessed by western blotting, confirming that Cdk13 and Cdk12 were comparably depleted (Figure 7A). siRNA-mediated knockdown of both kinases resulted in change of expression of hundreds of genes (>1.4-fold with $p < 0.05$) (Figure 7B). Namely, depletion of Cdk13 diminished expression of 250 genes and increased expression of 242 genes, while knockdown of Cdk12 downregulated 726 and upregulated 435 genes. For a list of all the down- and upregulated genes, see Table S2.

To probe the gene expression changes after Cdk12 knockdown, we selected three downregulated and two upregulated genes from the expression microarray data for further analysis. Cdk12 or Cdk13 were depleted by siRNA in HCT116 cells as shown by western blot analysis (Figure S6A). The qRT-PCR experiment confirmed the same expression pattern for Cdk12 depletion as observed in the microarray experiment, whereas no significant change was seen upon Cdk13 depletion (Figure S6B). Likewise, efficient depletion of Cdk13 from cells (Figure S7A) led to decrease of mRNA levels in three out of four selected genes found downregulated in the microarray (Figure S7B, upper panel), while two out of the three selected genes found upregulated in the microarray assay were modestly upregulated in qRT-PCR (Figure S7B, lower panel). To validate the dependence of the randomly selected transcripts on Cdk13 activity a rescue experiment was performed. Cells were depleted of

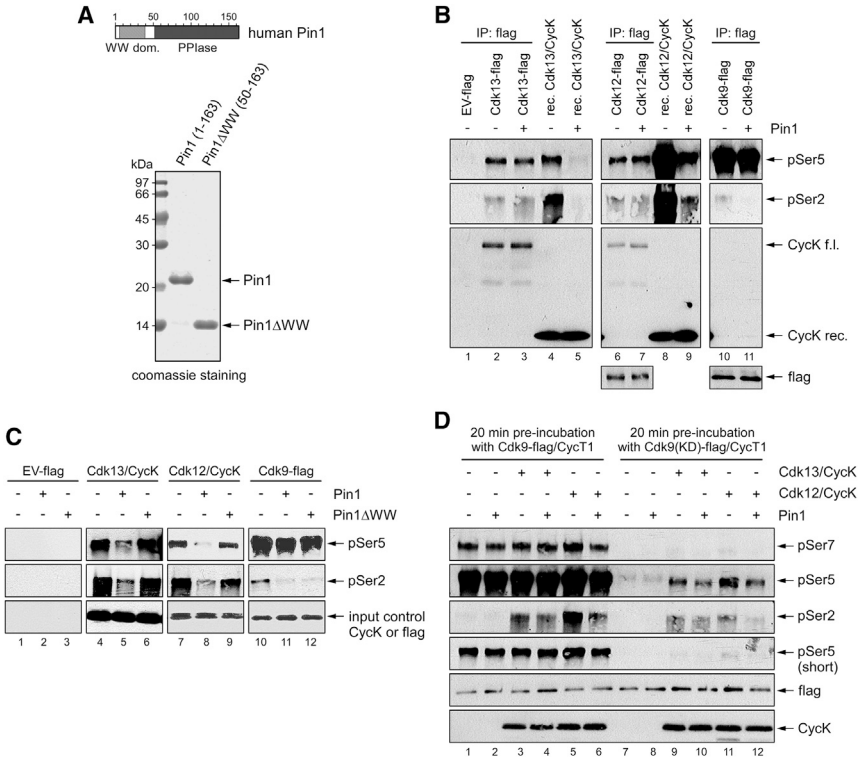

Figure 6. Pin1 Does Not Change the Phosphorylation Preferences of Cdk13/CycK

(A) The human peptidyl-prolyl isomerase Pin1 consists of an N-terminal WW domain followed by the isomerase domain. Full-length Pin1 (1–163) and a variant missing the N-terminal WW domain (Pin1ΔWW, 50–163) was generated.

(B) Phosphorylation preferences of transcription kinases Cdk13, Cdk12, and Cdk9, comparing flag-tagged immunoprecipitated full-length Cdk/cyclin proteins with recombinant protein complexes. Pin1 was optionally added in all kinase reactions. The protein input using an anti-CycK antibody or an anti-flag antibody is shown in the lower panels.

(C) The decrease of phosphorylation efficacy of recombinant Cdk13/CycK and Cdk12/CycK depends on the WW domain in Pin1. Whereas full Pin1 reduced the phosphorylation profiles of the recombinant kinases, deletion of the WW domain abrogated this ability. Such effect was not seen for flag-tagged Cdk9.

(D) Pre-incubation of the CTD with Cdk9/CycT1 leads to slightly increased Ser2 phosphorylations. A 20-min pre-incubation period of the CTD with Cdk9/CycT1 shows the expected Ser5/Ser7 phosphorylations (lanes 1 and 2). Administration of Cdk13/CycK or Cdk12/CycK leads to additional pSer2 marks (lanes 3–6). The same treatment using a kinase dead Cdk9 mutant shows significantly lower Ser2 phosphorylation levels (lanes 7–12). Addition of Pin1 only slightly reduced the phosphorylation signals of Cdk13 and Cdk12.

Cdk13 by a single siRNA and after 30 hr expression of Cdk13 was either rescued or not by transfection of a Cdk13 siRNA-insensitive plasmid. The efficacy of Cdk13 knockdown and rescue is showed by western blotting (Figure S7C). qRT-PCR results confirmed downregulation of all select mRNAs (Figure S7D), and rescue of Cdk13 expression resulted in increased expression of three out of four mRNAs.

To determine whether similar sets of genes and biological processes were affected upon the knockdown of Cdk13 and Cdk12, we analyzed the overlap between down- or upregulated genes for both kinases and performed gene ontology (GO) enrichment analyses of affected genes using the DAVID software. Depletion of Cdk13 and Cdk12 led to downregulation of largely different sets of genes with common downregulation of only 62 genes (Figure 7C, see Venn diagram on the left). Consistent with published work (Blazek et al., 2011; Bartkowiak and Greenleaf, 2015; Liang et al., 2015), GO analysis of genes downregulated upon Cdk12 knockdown indicated those genes to be enriched in processes related to DNA replication and repair (Figure 7C, upper bar graphs). In contrast, the GO analysis of Cdk13-dependent genes showed enrichment of functions connected to various extracellular and growth signaling pathways (Figure 7C, middle bar graphs). Genes with lowered expression upon both, Cdk12 and Cdk13, knockdowns are directing basic biological processes such as regulation of phosphatase activity and glycerolipid metabolism (Figure 7C, lower bar graphs). The analyses of upregulated genes are consistent with the finding that mostly different sets of genes and biological processes are regulated by both kinases (Figure 7D). Only 49 genes were commonly upregulated when either Cdk12 or Cdk13 was depleted; otherwise, different genes increased their expression (Figure 7D). Concomitantly, the upregulated genes for both kinases were enriched in different biological processes with the exception of their role in neuron development (Figure 7D, see bar graphs on the right) in line with findings of a recent study (Chen et al., 2014b). Together, the expression array and bioinformatics analyses show that Cdk12 and Cdk13 regulate expression of a markedly different set of genes that regulate dissimilar biological processes in human cells.

DISCUSSION

Cdk13 contains a C-terminal extension helix following the kinase domain that interacts with the ribose of the bound ATP through water-mediated contacts. A similar mode of interaction has been found for Cdk12 and Cdk9 (Bösken et al., 2014; Baumli et al., 2012), suggesting this conformation a molecular feature of transcription elongation regulating kinases. A polybasic cluster of six positively charged residues (KKRRRQK) and an aromatic residue followed by a glutamic acid (HE) constitute the conserved motifs of the extension helix in Cdk13. The association of the basic patch in close proximity to the ATP binding site could facilitate an electrostatic association to the highly negatively charged RNAPII CTD and potentially also define a register for the association of the phosphate groups within the structure of the CTD (Figure S2). The extension segment also creates a unique means for the specific interaction with potential inhibitors. Superimposition of the structure of Cdk13·ADP with

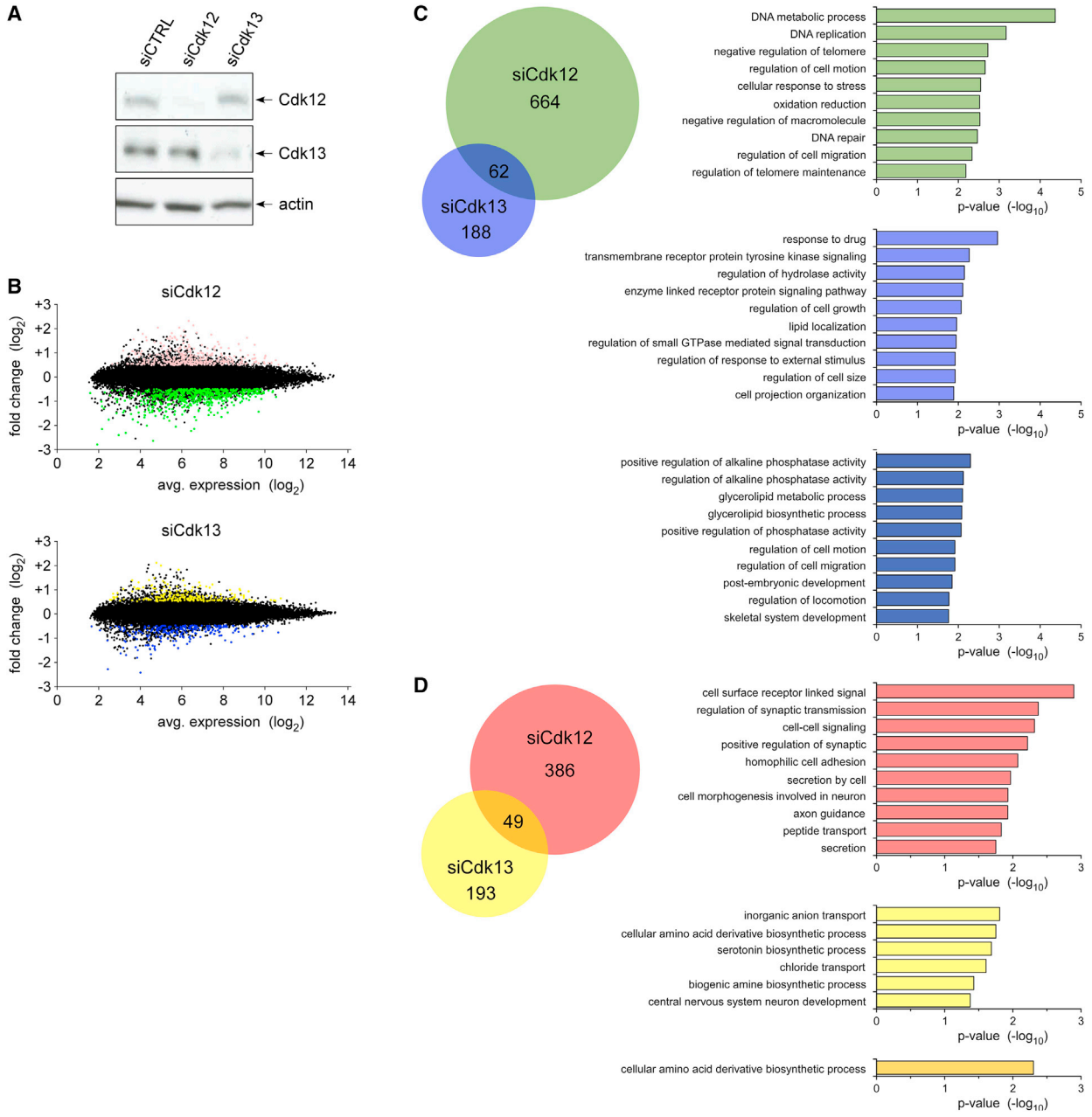

Figure 7. Knockdown of Cdk12 or Cdk13 Exhibits Different Gene Expression Profiles

(A) Knockdown efficacy of Cdk12 and Cdk13. Anti-Cdk12 and -Cdk13 antibodies show the expression levels of these kinases together with an actin antibody as loading control.

(B) Genes that were differentially regulated after siRNA knockdown of Cdk12 (siCdk12) or Cdk13 (siCdk13) in HCT116 cells were determined by expression microarray. Relative average expression levels of genes (x axis, $\log_2$) are plotted against their fold change (knockdown/control, y axis, $\log_2$). Significantly downregulated genes (>1.4-fold, $p < 0.05$) or upregulated genes (>1.4-fold, $p < 0.05$) are indicated for Cdk12 knockdown in the left graph (downregulated, green; upregulated, red) and for Cdk13 knockdown in the right graph (downregulated, blue; upregulated, yellow).

(C) The overlap in altered genes between Cdk12 and Cdk13 knockdown was examined (Venn diagram, left panel). Biological processes in which altered genes are involved were determined by GO enrichment analysis (DAVID, EASE threshold 0.05). The ten most significantly represented biological processes are summarized in bar graphs for Cdk12 knockdown (upper panel, green), for Cdk13 knockdown (middle panel, blue), or for genes that were similarly downregulated (lower panel, purple). The x axis indicates the $-\log_{10}$ p value.

(D) The same analysis was performed for genes that were significantly upregulated (>1.4-fold, $p < 0.05$) after siRNA-mediated knockdown of Cdk12 (red) or Cdk13 (yellow). The overlap of altered genes for each knockdown was determined (Venn diagram, left). The top most significantly represented biological processes are show for Cdk12 knockdown (red bars), for Cdk13 knockdown (yellow bars), or genes that were similarly upregulated after Cdk12 and Cdk13 knockdown (orange bar).

Cdk9•flavopiridol shows a steric clash of H1018 of the Cdk13 HE motif with a benzol ring of flavopiridol (Figure 5). A compound designed to mediate direct hydrogen bond interactions with the HE residues of Cdk13 might instead exhibit a higher binding affinity to this kinase and a higher specificity of inhibition. Of note, the crystal structure of Cdk9 in complex with flavopiridol (Baumli et al., 2008) (PDB: 3BLR) was determined with a C-terminally truncated protein variant, missing the FE motif in Cdk9 and the polybasic cluster.

The coordination of the phosphorylated threonine in the kinase T-loop emerges as another specific feature of transcription regulating CDKs. The formation of three salt bridges between arginine residues from sequentially distant loop sections of the kinase to the phosphorylated threonine of the T-loop is a hallmark of CDK activation (Johnson and Lewis, 2001). These salt bridges lead to stabilization of the loop sections, mostly the T-loop, a twist of the DFGxxR motif, the positioning of the catalytic aspartate from the HRD motif, and a re-orientation of the C-helix that contains the PITAIRE motif (Figures 1 and 2). Intriguingly, the third canonical salt bridge between the R from the PITAIRE motif and the pT is not formed in either Cdk13 or Cdk12 (Figure 3). Instead, a salt bridge is formed between the arginine and the second glutamic acid of the KVEE motif, giving room for the association of substrate residues.

The regulation of Cdk13 activity is not well understood today as the expression levels of the corresponding cyclin subunit, CycK, are rather stable. This is similar to other cyclins controlling transcriptional CDKs, e.g., CycT1, but different from cell-cycle-regulating cyclins such as CycA. The Cdk13 kinase is unusually large with 690 residues preceding the kinase domain and 510 residues following the kinase domain. Regulation steps could possibly be mediated by cellular localization or by intra-molecular interactions, e.g., via the N-terminal SR elements. Despite being involved in constitutive and alternative splicing events, SR proteins are thought to attach to newly made pre-mRNA to prevent the pre-mRNA from binding to the coding DNA strand to increase genome stabilization (Zhou and Fu, 2013).

The peptidyl-prolyl isomerase Pin1 does not change the phosphorylation preferences of the transcription elongation kinases Cdk9, Cdk12, and Cdk13 (Figure 6). Using recombinant proteins or flag-tag immuno-precipitated full-length proteins with the corresponding cyclin subunits, we could not see any shift toward increased Ser2 phosphorylation levels of the CTD. Likewise, the activity of the kinases is not changed upon the presence of Pin1. This result is similar to the recently published observation that the Pin1 ortholog Ess1 from yeast does not stimulate the activity of Cdk12 (Bartkowiak and Greenleaf, 2015). Whereas writing of the CTD phosphorylations is not influenced by the isomerase, dephosphorylation by the CTD phosphatase Fcp1 was shown to be modulated by Pin1 (Xu et al., 2003). Hyper-phosphorylation of the CTD thus correlates with the inhibition of Fcp1 by Pin1, whose activity is high in early stages of the transcription cycle (Xu and Manley, 2007). Yet, pre-incubation of the CTD with Cdk9/CycT1 resulting in a strong Ser5 phosphorylation signal led to a small increase in pSer2 marks after exposure to either Cdk12 or Cdk13.

Despite the fact that Cdk13 and Cdk12 have similar kinase domains and share the same regulating cyclin, both kinases regulate expression of a largely different set of genes and biological processes. Consistent with our expression analyses are results of a recent study showing that Cdk12 knockout leads to an early post-implantation embryonal lethality in mice pointing to a very specific and non-redundant role of Cdk13 and Cdk12 in development perhaps by the regulation of expression of different gene sets (Chen et al., 2014b). Notably, the same study showed that Cdk13 and Cdk12 regulate also expression of a common gene, Cdk5, to direct axonal growth. The gene expression profiles are also consistent with a prominent role of Cdk12 in the expression of the c-FOS proto-oncogene induced by the epidermal growth factor (Eifler et al., 2015). Further evidence pointing to different function of both kinases was provided by knockdown of Cdk13 and Cdk12 in embryonic stem cells, which resulted in differentiation via regulation of expression of different sets of genes (Dai et al., 2012).

Cyclin-dependent kinases have evolved as important target proteins for the treatment of multiple diseases, including cancer and leukemia (Malumbres and Barbacid, 2009). Despite the Cdk/cyclin pairs driving the cell cycle (interphase regulating Cdk2, Cdk4, and Cdk6, and mitotic Cdk5), transcriptional CDKs 7, 8, 9, 12, and 13 are now increasingly recognized as important factors of tumor oncogenesis. Discovery of a covalent Cdk7 inhibitor targeting a cysteine residue outside the canonical kinase domain provided an unanticipated means of achieving selectivity (Kwiatkowski et al., 2014). Inhibition of Cdk9 activity has been identified as another means to counteract cancer cell progression, mixed lineage leukemia, and HIV (Wang and Fischer, 2008). With the crystal structure of Cdk13/CycK determined, we provide the structural basis for targeted drug discovery against this human kinase.

EXPERIMENTAL PROCEDURES

Plasmids and Proteins

Cdk13/CycK proteins were expressed in baculo-virus-infected *Sf9* cells and purified as described in the Supplemental Experimental Procedures.

Crystallization and Structure Determination

For crystallization, the purified Cdk13/CycK complex was mixed at 85 μM concentration with ADP, AlF_3, $MgCl_2$ and substrate peptide P-pS-YSPTSP-pS-YSPT in molar ratios of 1:8:32:64:8 and incubated on ice for 30 min. Initial crystals were obtained using the hanging drop vapor diffusion technique at 293 K. The crystal structure was determined and refined as described in the Supplemental Experimental Procedures and Table S1.

RNA Polymerase II CTD Substrate Peptides

For kinase activity analyses, various CTD polypeptides were purchased from Biosyntan or synthesized in house with 95% purity (high-performance liquid chromatography [HPLC] grade). The peptide used for crystallization (ac-P-pS-YSPTSP-pS-YSPT-amid) contained two phosphorylated serine residues at heptad position 7. For quantitative analysis in electrospray ionization mass spectrometry (ESI-MS) experiments or radioactive filter-binding assays, CTD substrate peptides were marked at the C terminus with a double arginine motif separated by a polyethylene glycol spacer. The arginines were set for improved transfer rates in quantitative filter binding assays and for improved ionization properties in ESI-MS analyses.

In Vitro Kinase Assays

Radioactive kinase reactions (typically 35 μl) were carried out with recombinant, highly purified proteins using a standard protocol. In short, Cdk13/CycK (0.2–0.5 μM) was pre-incubated with CTD substrates (peptides 100 μM; GST-CTD full length [f.l.] 10 μM) for 5–10 min at room temperature

in kinase buffer (150 mM HEPES [pH 7.6], 34 mM KCl, 7 mM $MgCl_2$, 2.5 mM dithiothreitol, 5 mM β-glycerol phosphate, 1 × PhosSTOP [Roche]). Cold ATP (to a final concentration of 1–2 mM) and 3 μCi [^{32}P]-γ-ATP (Perkin-Elmer) were added, and the reaction mixture was incubated up to 30 min at 30°C at 350 rpm. Reactions were stopped by adding EDTA to a final concentration of 50 mM. For reactions using GST-CTD, aliquots of 11 μl each were spotted onto P81 Whatman paper squares. For substrate peptides, Optitran BA-S85 reinforced membrane was used. Paper squares were washed three times for 5 min with 0.75% (v/v) phosphoric acid, with at least 5 ml washing solution per paper. Radioactivity was counted in a Beckman Scintillation Counter (Beckman Coulter) for 1 min. Measurements were performed in triplicate and are represented as mean with SD.

Kinase Assays with Flag-Tagged Proteins

Plasmids of full-length flag-tagged proteins, immuno-precipitations from cell lysate, and kinase assays are described in the Supplemental Experimental Procedures.

Short Interference RNA Transfections and Flavopiridol Treatment

HCT116 cells were plated at 20% confluency in 6-well plates in culture medium without antibiotics. After 24 hr cultivation, transfections using Cdk12, Cdk13 or control siRNA (Santa Cruz Biotechnology) were performed or cells were just mock transfected. The transfections were done in a total volume of 2.5 ml containing 2.5 μl of 10 μM siRNA and 5 μl of Lipofectamine RNAiMax (Invitrogene) according to the manufacturer's instructions. Transfection mix was removed 3 hr later, and cells were grown for another 69 hr in fresh media. Mock-transfected cells were treated with flavopiridol (500 nM final concentration) 2 hr prior the cell harvest. Then, cells were lysed in buffer containing 20 mM HEPES/KOH (pH 7.9), 15% glycerol, 0.2% NP-40, 150 mM KCl, 1 mM DTT, 0.2 mM EDTA, and protease inhibitor (Sigma), and the CTD phosphorylations were analyzed by western blotting with phospho-specific antibodies.

Western Blots

For western blot analysis, kinase assays were run with 0.2 μM Cdk13/CycK, 0.2 μM Cdk12/CycK, 5 μM Pin1, 5 μM Pin1ΔWW, 10 μM GST-CTD f.l., and 2 mM ATP in kinase buffer. After incubation with Cdk13/CycK, GST-CTD proteins were subjected to SDS-PAGE on a 12% gel before transfer to nitrocellulose (GE Healthcare). Monoclonal antibodies specific for RNAPII CTD phosphorylation sites pSer2 (3E10), pSer5 (3E8), and pSer7 (4E12) were used as described previously (Bösken et al., 2014). Membranes were stained with chicken anti-rat immunoglobulin G (IgG) horseradish peroxidase (HRP) secondary antibodies, and antibody recognition was revealed by enhanced chemiluminescence.

Expression Microarrays

For expression microarrays HCT116 cells were transfected in triplicate with 1 μl of 10 μM CTRL, Cdk12, and Cdk13 siRNAs as described above. After 72 hr, cells were harvested and RNA isolated with miRNAeasy kit (QIAGEN) according to the manufacturer's instructions. A total of nine samples was used: three from the siRNA CTRL, three from siRNA Cdk12, and three from siRNA Cdk13 knockdowns. Human Gene 1.0ST microarrays from Affymetrix were used. Details on sample preparation and data analyses are provided in the Supplemental Information.

ACCESSION NUMBERS

Structure coordinates and diffraction data of the Cdk13/CycK complex were deposited in the Protein Data Bank (http://www.pdb.org) under accession code PDB: 5EFQ.

SUPPLEMENTAL INFORMATION

Supplemental Information includes Supplemental Experimental Procedures, seven figures, and two tables and can be found with this article online at http://dx.doi.org/10.1016/j.celrep.2015.12.025.

AUTHOR CONTRIBUTIONS

A.K.G. expressed and purified the proteins and performed the biochemical activity assays. D.H. crystallized the proteins with the help of C.A.B. and determined the structure together with C.A.B. and K.A. Kinase activity measurements with flag-tagged proteins and gene ontology studies were performed by K.P. and K.B. under the supervision of D.B. Experiments with Pin1 were performed by R.D. M.G. designed the study and wrote the manuscript with support of D.B. All authors discussed the results and commented on the manuscript.

ACKNOWLEDGMENTS

We thank Karin Vogel-Bachmayr and Sascha Gentz for excellent technical assistance, Ingrid Vetter for help with crystal data evaluation, the beamline staff at the SLS Villigen, Switzerland, for help with data collection, and Pavla Gajdušková for cloning flag-tagged expression constructs. Microarray profiling was performed at the Gladstone Genomics Core and statistical analysis of the microarray data was conducted by Alex Williams at the Gladstone Bioinformatics Core. M.G. is a member of the DFG excellence cluster ImmunoSensation. D.B. is supported by a project "CEITEC – Central European Institute of Technology" (CZ.1.05/1.1.00/02.0068) and a GACR grant (14-09979S). This work was supported by a grant from the Deutsche Forschungsgemeinschaft to M.G. (GE 976/9-1).

Received: July 7, 2015
Revised: October 29, 2015
Accepted: November 30, 2015
Published: December 31, 2015

REFERENCES

Adelman, K., and Lis, J.T. (2012). Promoter-proximal pausing of RNA polymerase II: emerging roles in metazoans. Nat. Rev. Genet. *13*, 720–731.

Allen, B.L., and Taatjes, D.J. (2015). The Mediator complex: a central integrator of transcription. Nat. Rev. Mol. Cell Biol. *16*, 155–166.

Bartkowiak, B., and Greenleaf, A.L. (2015). Expression, purification, and identification of associated proteins of the full-length hCDK12/CyclinK complex. J. Biol. Chem. *290*, 1786–1795.

Bartkowiak, B., Liu, P., Phatnani, H.P., Fuda, N.J., Cooper, J.J., Price, D.H., Adelman, K., Lis, J.T., and Greenleaf, A.L. (2010). CDK12 is a transcription elongation-associated CTD kinase, the metazoan ortholog of yeast Ctk1. Genes Dev. *24*, 2303–2316.

Baumli, S., Lolli, G., Lowe, E.D., Troiani, S., Rusconi, L., Bullock, A.N., Debreczeni, J.E., Knapp, S., and Johnson, L.N. (2008). The structure of P-TEFb (CDK9/cyclin T1), its complex with flavopiridol and regulation by phosphorylation. EMBO J. *27*, 1907–1918.

Baumli, S., Hole, A.J., Wang, L.Z., Noble, M.E., and Endicott, J.A. (2012). The CDK9 tail determines the reaction pathway of positive transcription elongation factor b. Structure *20*, 1788–1795.

Berro, R., Pedati, C., Kehn-Hall, K., Wu, W., Klase, Z., Even, Y., Geneviève, A.M., Ammosova, T., Nekhai, S., and Kashanchi, F. (2008). CDK13, a new potential human immunodeficiency virus type 1 inhibitory factor regulating viral mRNA splicing. J. Virol. *82*, 7155–7166.

Blazek, D., Kohoutek, J., Bartholomeeusen, K., Johansen, E., Hulinkova, P., Luo, Z., Cimermancic, P., Ule, J., and Peterlin, B.M. (2011). The Cyclin K/Cdk12 complex maintains genomic stability via regulation of expression of DNA damage response genes. Genes Dev. *25*, 2158–2172.

Bösken, C.A., Farnung, L., Hintermair, C., Merzel Schachter, M., Vogel-Bachmayr, K., Blazek, D., Anand, K., Fisher, R.P., Eick, D., and Geyer, M. (2014). The structure and substrate specificity of human Cdk12/Cyclin K. Nat. Commun. *5*, 3505.

Buratowski, S. (2009). Progression through the RNA polymerase II CTD cycle. Mol. Cell *36*, 541–546.

The Cancer Genome Atlas Research Network (2011). Integrated genomic analyses of ovarian carcinoma. Nature *474*, 609–615.

Chen, C., Ha, B.H., Thévenin, A.F., Lou, H.J., Zhang, R., Yip, K.Y., Peterson, J.R., Gerstein, M., Kim, P.M., Filippakopoulos, P., et al. (2014a). Identification of a major determinant for serine-threonine kinase phosphoacceptor specificity. Mol. Cell *53*, 140–147.

Chen, H.R., Lin, G.T., Huang, C.K., and Fann, M.J. (2014b). Cdk12 and Cdk13 regulate axonal elongation through a common signaling pathway that modulates Cdk5 expression. Exp. Neurol. *261*, 10–21.

Corden, J.L. (2013). RNA polymerase II C-terminal domain: Tethering transcription to transcript and template. Chem. Rev. *113*, 8423–8455.

Czudnochowski, N., Bösken, C.A., and Geyer, M. (2012). Serine-7 but not serine-5 phosphorylation primes RNA polymerase II CTD for P-TEFb recognition. Nat. Commun. *3*, 842.

Dai, Q., Lei, T., Zhao, C., Zhong, J., Tang, Y.Z., Chen, B., Yang, J., Li, C., Wang, S., Song, X., et al. (2012). Cyclin K-containing kinase complexes maintain self-renewal in murine embryonic stem cells. J. Biol. Chem. *287*, 25344–25352.

Davidson, L., Muniz, L., and West, S. (2014). 3′ end formation of pre-mRNA and phosphorylation of Ser2 on the RNA polymerase II CTD are reciprocally coupled in human cells. Genes Dev. *28*, 342–356.

Eick, D., and Geyer, M. (2013). The RNA polymerase II carboxy-terminal domain (CTD) code. Chem. Rev. *113*, 8456–8490.

Eifler, T.T., Shao, W., Bartholomeeusen, K., Fujinaga, K., Jäger, S., Johnson, J.R., Luo, Z., Krogan, N.J., and Peterlin, B.M. (2015). Cyclin-dependent kinase 12 increases 3′ end processing of growth factor-induced c-FOS transcripts. Mol. Cell. Biol. *35*, 468–478.

Ekumi, K.M., Paculova, H., Lenasi, T., Pospichalova, V., Bösken, C.A., Rybarikova, J., Bryja, V., Geyer, M., Blazek, D., and Barboric, M. (2015). Ovarian carcinoma CDK12 mutations misregulate expression of DNA repair genes via deficient formation and function of the Cdk12/CycK complex. Nucleic Acids Res. *43*, 2575–2589.

Ghamari, A., van de Corput, M.P., Thongjuea, S., van Cappellen, W.A., van Ijcken, W., van Haren, J., Soler, E., Eick, D., Lenhard, B., and Grosveld, F.G. (2013). *In vivo* live imaging of RNA polymerase II transcription factories in primary cells. Genes Dev. *27*, 767–777.

Ghosh, G., and Adams, J.A. (2011). Phosphorylation mechanism and structure of serine-arginine protein kinases. FEBS J. *278*, 587–597.

Grünberg, S., and Hahn, S. (2013). Structural insights into transcription initiation by RNA polymerase II. Trends Biochem. Sci. *38*, 603–611.

Hanes, S.D. (2014). The Ess1 prolyl isomerase: traffic cop of the RNA polymerase II transcription cycle. Biochim. Biophys. Acta *1839*, 316–333.

Itzen, F., Greifenberg, A.K., Bösken, C.A., and Geyer, M. (2014). Brd4 activates P-TEFb for RNA polymerase II CTD phosphorylation. Nucleic Acids Res. *42*, 7577–7590.

Kwiatkowski, N., Zhang, T., Rahl, P.B., Abraham, B.J., Reddy, J., Ficarro, S.B., Dastur, A., Amzallag, A., Ramaswamy, S., Tesar, B., et al. (2014). Targeting transcription regulation in cancer with a covalent CDK7 inhibitor. Nature *511*, 616–620.

Johnson, L.N., and Lewis, R.J. (2001). Structural basis for control by phosphorylation. Chem. Rev. *101*, 2209–2242.

Joshi, P.M., Sutor, S.L., Huntoon, C.J., and Karnitz, L.M. (2014). Ovarian cancer-associated mutations disable catalytic activity of CDK12, a kinase that promotes homologous recombination repair and resistance to cisplatin and poly(ADP-ribose) polymerase inhibitors. J. Biol. Chem. *289*, 9247–9253.

Larochelle, S., Amat, R., Glover-Cutter, K., Sansó, M., Zhang, C., Allen, J.J., Shokat, K.M., Bentley, D.L., and Fisher, R.P. (2012). Cyclin-dependent kinase control of the initiation-to-elongation switch of RNA polymerase II. Nat. Struct. Mol. Biol. *19*, 1108–1115.

Liang, K., Gao, X., Gilmore, J.M., Florens, L., Washburn, M.P., Smith, E., and Shilatifard, A. (2015). Characterization of human cyclin-dependent kinase 12 (CDK12) and CDK13 complexes in C-terminal domain phosphorylation, gene transcription, and RNA processing. Mol. Cell. Biol. *35*, 928–938.

Malumbres, M., and Barbacid, M. (2009). Cell cycle, CDKs and cancer: a changing paradigm. Nat. Rev. Cancer *9*, 153–166.

Peterlin, B.M., and Price, D.H. (2006). Controlling the elongation phase of transcription with P-TEFb. Mol. Cell *23*, 297–305.

Russo, A.A., Jeffrey, P.D., and Pavletich, N.P. (1996). Structural basis of cyclin-dependent kinase activation by phosphorylation. Nat. Struct. Biol. *3*, 696–700.

Schiene-Fischer, C., Aumüller, T., and Fischer, G. (2013). Peptide bond cis/trans isomerases: a biocatalysis perspective of conformational dynamics in proteins. Top. Curr. Chem. *328*, 35–67.

Schulze-Gahmen, U., Upton, H., Birnberg, A., Bao, K., Chou, S., Krogan, N.J., Zhou, Q., and Alber, T. (2013). The AFF4 scaffold binds human P-TEFb adjacent to HIV Tat. eLife *2*, e00327.

St Amour, C.V., Sansó, M., Bösken, C.A., Lee, K.M., Larochelle, S., Zhang, C., Shokat, K.M., Geyer, M., and Fisher, R.P. (2012). Separate domains of fission yeast Cdk9 (P-TEFb) are required for capping enzyme recruitment and primed (Ser7-phosphorylated) Rpb1 carboxyl-terminal domain substrate recognition. Mol. Cell. Biol. *32*, 2372–2383.

Wang, S., and Fischer, P.M. (2008). Cyclin-dependent kinase 9: a key transcriptional regulator and potential drug target in oncology, virology and cardiology. Trends Pharmacol. Sci. *29*, 302–313.

Xu, Y.X., and Manley, J.L. (2007). Pin1 modulates RNA polymerase II activity during the transcription cycle. Genes Dev. *21*, 2950–2962.

Xu, Y.X., Hirose, Y., Zhou, X.Z., Lu, K.P., and Manley, J.L. (2003). Pin1 modulates the structure and function of human RNA polymerase II. Genes Dev. *17*, 2765–2776.

Zhou, Z., and Fu, X.D. (2013). Regulation of splicing by SR proteins and SR protein-specific kinases. Chromosoma *122*, 191–207.